2 Newtonian fluid mechanics

R.M. NEDDERMAN

Introduction

The previous chapter has shown how plant flowsheets can be constructed and analysed, and how the viability of a project approximately can be costed. In the flowsheets discussed in Chapter 1, no account was made of how food material moves from one plant unit to another. The next stage of design is to make accurate estimates of the size of these units and of the flows between them. The prediction of the way fluids flow is vital in engineering design, for example in the calculation of pipe sizes and pump duties. It is also necessary to have some idea of the history of the fluid during processing; in food systems, as will be seen later, the range of velocities in the flow can affect the amount and range of thermal processing a fluid receives, and thus can affect the safety and quality of the final product.

The study of fluid flow has to be firmly based on physical principles, such as the conservation of energy and momentum, and on sound physical models for the fluid itself. For fluids such as air and water, the science of fluid mechanics is well developed. Food fluids are much more complex, as will be seen in Chapters 5 and 10, but are ruled by the same principles. This chapter outlines the principles, using examples from simple fluids to make the mathematics clear. It is important to be able to distinguish between turbulent and laminar flows; this chapter describes the characteristics of both. Many flowing food fluids are essentially laminar, although their flows are more complex than those of the Newtonian fluids discussed here. The idea of laminar flows is extended to the study of more complex fluids in Chapter 5. One key idea which is introduced here is that of dynamic similarity. If flows have the same characteristics, then experiments carried out in a given geometry at one scale will be representative of results on other scales. There is still no accurate physical model for many practical situations, so the idea of dynamic similarity is invaluable; it allows correlations to be developed for quantities such as pressure drop and heat transfer coefficient in terms of dimensionless groups, which can then be applied to any length scale of equipment. Many such correlations will be seen throughout this book.

Chemical Engineering for the Food Industry. Edited by P.J. Fryer, D.L. Pyle and C.D. Rielly. Published in 1997 by Blackie A & P, an imprint of Chapman & Hall, London. ISBN 0 412 49500 7

2.1 Laminar and turbulent flow

2.1.1 Introduction

Many of the more important processes of the food industry – heating, mixing and transportation – depend on the fluid properties of the food material or its surroundings. Fluid mechanics therefore underpins much of food technology, and the purpose of this chapter is to form a foundation on which subsequent chapters can build.

Food fluids are generally complex and have a flow behaviour that depends both on their structure and on their processing history. Predicting the flow is therefore difficult. However, the principles that govern the flow behaviour of foods are the same as those that describe the flow of simple fluids such as water. This chapter therefore considers the flow of simple Newtonian fluids; more complex materials will be considered later in Chapters 5 and 10.

At low speeds, fluids tend to flow in a steady and reproducible manner. Such flows are said to be **laminar**, as one layer (lamina) flows smoothly over another. Laminar flows are also called **viscous** flows, as viscous forces (see section 2.3) dominate under these conditions. At higher speeds random eddies occur in the fluid and the flow is said to be **turbulent**. The eddies in turbulent flow have a range of sizes, but the average eddy size is often small compared with the size of the duct along which the fluid is flowing. Under these circumstances the velocity fluctuates randomly about a well-defined mean with only a small variation between maximum and minimum values. Sometimes, however, large eddies occur giving widely fluctuating velocities, and it becomes difficult to define a mean velocity. The distinction between these two types of turbulent flow can be appreciated by comparing the flow produced by a fan, with the wind on a gusty day. Figure 2.1 illustrates the variation of the velocity at a point with time in these three situations.

The behaviour of laminar flows can often be predicted from purely theoretical considerations. However, the theory of turbulent flow is less well advanced, and we usually have to resort to correlations of experimental results to predict the behaviour of fluids under these conditions.

2.1.2 Critical Reynolds numbers

In a pipe of diameter D, the transition from laminar to turbulent flow is found to be sudden; it occurs when the group $v_m D\rho/\mu$ equals about 2200, where v_m is the mean velocity of the fluid and ρ and μ are its density and viscosity. This group is known as the **Reynolds number**, after the discoverer of this phenomenon. Each geometry has its own critical Reynolds number, and the value of 2200 is specific for pipes of circular cross-section. Though we have said that the transition is sudden at the critical Reynolds number,

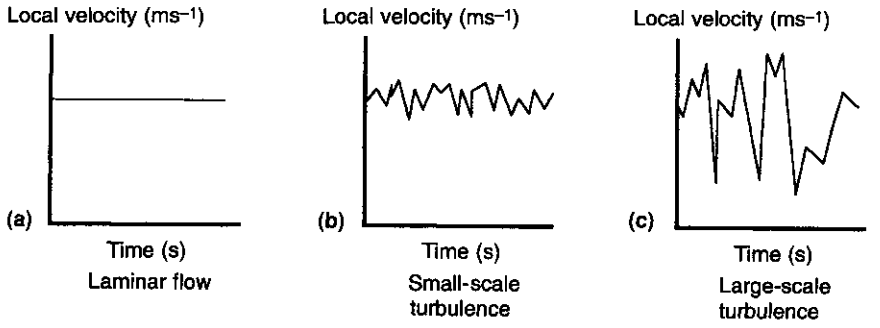

Fig. 2.1 Variation of velocity at a point in different types of flow: (a) laminar; (b) small-scale turbulence; (c) large-scale turbulence.

the behaviour close to that value tends to be unreproducible. Thus it is not always possible to say whether a flow in the Reynolds number range 2000–2400 will be laminar or turbulent, and sometimes it is found that the behaviour switches irregularly between these two states.

2.1.3 Velocity profiles

In laminar pipe flow, it can be shown theoretically (section 2.3) that the velocity profile is parabolic and given by

$$v = v_1\left[1 - \left(\frac{r}{R}\right)^2\right] \tag{2.1}$$

where v is the velocity at radius r and R is the radius of the pipe, i.e. $D/2$.

In turbulent flow the velocity distribution is well correlated by the so-called **one-seventh power law**, discussed further in section 2.5.6:

$$v = v_1\left(\frac{y}{R}\right)^{1/7} = \frac{60}{49}v_m\left(\frac{y}{R}\right)^{1/7} \tag{2.2}$$

where v_1 is the centreline velocity, v_m is the mean velocity and y is the distance from the wall, i.e. $y = R - r$.

These profiles are plotted in Fig. 2.2 for the same flowrate. It can be seen that in turbulent flow the velocity is much more uniform than in laminar flow, as a result of the mixing action of the eddies. In laminar flow the centreline velocity is twice the mean velocity, while in turbulent flow the centreline velocity is only 60/49 = 1.22 times the mean. This has implications for the design of continuous sterilizers, discussed in later sections.

Food fluids generally have high viscosities and thus their flow tends to be laminar. However, in many cases they also show non-Newtonian behaviour

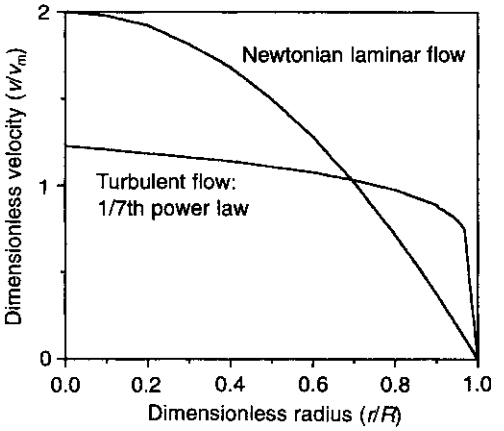

Fig. 2.2 Comparison of velocity profiles in pipe flow.

– that is, variable viscosity – and this will be discussed in Chapter 5. However, there are several low-viscosity fluids of importance in the food industry, such as water and milk, for which the conventional fluid mechanics outlined in this chapter is relevant. Furthermore, a study of these simple fluids provides a firm foundation on which the study of non-Newtonian fluids is traditionally based.

2.1.4 Pressure

It is appropriate at this stage to discuss the concept of **pressure**. This is the force per unit area exerted by the fluid, and acts equally in all directions. In a stationary fluid the pressure increases linearly with depth at a rate ρg where ρ is the density and g the acceleration due to gravity. This result provides a simple means of measuring pressure known as the U-tube manometer. This is a U-shaped tube partially filled with liquid of density ρ_m, with one end connected to the point of interest and the other open to the atmosphere, as shown in Fig. 2.3. The pressure at the measurement point is given by

$$P = P_a + \rho_m g h$$

where P_a is atmospheric pressure and h is the difference in height of the fluid in the two limbs. A U-tube manometer can also be used to measure pressure differences by connecting the two ends to two points of interest between which it is required to measure the pressure difference. Under these circumstances it becomes necessary to make allowance for the weight of the fluid in the tube, and the pressure difference ΔP is given by

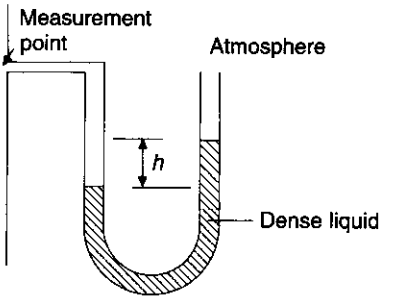

Fig. 2.3 The U-tube manometer.

$$\Delta P = (\rho_m - \rho_f) g h$$

where ρ_m is the density of the manometer liquid and ρ_f is the density of the flowing fluid.

2.2 Ideal fluids

2.2.1 Introduction

Considerable insight can often be gained into the behaviour of fluids in pipes and ducts by assuming that the fluid is ideal: that is, that the velocity is uniform across the duct and that the fluid has zero viscosity (viscosity is defined in section 2.3.1). Although no real fluid conforms to this ideal, these assumptions give rise to little error in many examples of practical importance. As we shall see later (for example, in section 2.5), these assumptions are best for short lengths of pipe. They are therefore appropriate for considering sudden changes such as changes in cross-section, or pipe bends. It can be seen from Fig. 2.2 that the assumption of uniform velocity is more appropriate for turbulent than for laminar flow.

Ideal fluid analysis is based on three basic conservation equations: the conservation of mass, energy and momentum. We shall apply these conservation laws over a short distance between two sections of a generalized duct, which are denoted by section 1 and 2 in Fig. 2.4. F is the force on the wall. The dotted line in this figure represents a **control surface**, which encloses the **control volume**, i.e. that part of the system to which we are paying attention. Very commonly in ideal flows we do not need to consider what happens within the control volume as we can obtain enough information by considering the properties of the fluid as it enters and leaves through the control surface. This is the same principle as that used in Chapter 1.

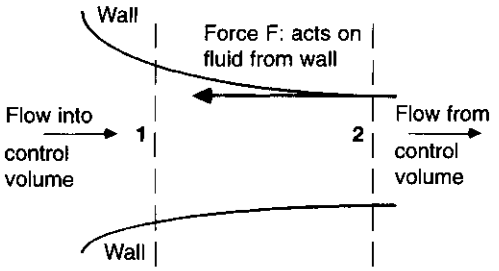

Fig. 2.4 A hypothetical duct. The dotted lines denote the edges of the control surface discussed in the text.

2.2.2 *Conservation of mass: the continuity equation*

If the velocity is constant across any cross-section in the duct, the mass flowrate w is given by

$$w = av\rho \tag{2.3}$$

where v is the velocity of the fluid, ρ is its density and A is the cross-sectional area of the duct. If we consider a duct of varying cross-section as in Fig. 2.4, we can say from the conservation of mass that w is a constant and therefore the flow into the system will equal the flow out in the absence of accumulation. Thus

$$w = A_1 v_1 \rho_1 = A_2 v_2 \rho_2 \tag{2.4}$$

where the subscripts 1 and 2 denote the conditions at the two selected sections.

2.2.3 *The conservation of energy: Bernoulli's equation*

The fluid entering the duct at section 1 of Fig. 2.4 will be subjected to a force equal to the product of the cross-sectional area and the pressure. The boundary dividing this fluid from the fluid behind it will have moved a distance x, and therefore the work done on the fluid entering the duct by the fluid behind it will be PAx, which equals P_1V_1, where P_1 is the pressure at section 1 and V_1 is the volume of fluid entering the duct. For unit mass entering the duct, V will be equal to the reciprocal of the density, i.e. $1/\rho$. Therefore the work done on a unit mass of the fluid entering the duct is P_1/ρ. Similarly, when the fluid leaves, it does work P_2/ρ on the fluid ahead. The fluid had kinetic energy $\frac{1}{2}v_1^2$ per unit mass on entering and has kinetic energy $\frac{1}{2}v_2^2$ on leaving. In the process the fluid has gained potential energy $g(h_2 - h_1)$, where h is height above some arbitrary datum. Assuming that the total energy is conserved between sections 1 and 2, we have as an expression of the conservation of energy

$$\frac{P_1}{\rho} + \frac{v_1^2}{2} + gh_1 = \frac{P_2}{\rho} + \frac{v_2^2}{2} + gh_2 \tag{2.5}$$

This energy balance is known as Bernoulli's equation. It is very useful in the study of flows. Various assumptions have been made in the derivation:

- that the density is constant;
- that the system operates in the steady state, as we have assumed that there is no accumulation of energy between sections 1 and 2;
- that there is no interchange between thermal and mechanical energy, i.e. that the internal energy and hence the temperature of the fluid does not change between sections 1 and 2.

As the two pressure terms in Bernoulli's equation are divided by the same density, we can use either the genuine thermodynamic pressure, known as the **absolute pressure**, or measure the pressure above an arbitrary datum. When measured above atmospheric pressure, the difference is known as the **gauge pressure**.

In low-speed flows, there is little possibility of thermal energy being converted into mechanical energy. However, the converse is possible, especially in the more grossly eddying turbulent flows, and in this case some of the mechanical energy is lost within the section. In all other circumstances a loss term must be included:

$$\frac{P_1}{\rho} + \frac{v_1^2}{2} + gh_1 = \frac{P_2}{\rho} + \frac{v_2^2}{2} + gh_2 + E_L \tag{2.6}$$

where E_L is the energy lost per unit mass between sections 1 and 2. Bernoulli's equation should only be used for the steady flow of constant-density fluids.

2.2.4 *Conservation of momentum: the momentum equation*

The momentum equation is based on Newton's second law, that the rate of change of momentum is equal to the net applied force. This is often expressed in the form

$$F = ma = m\frac{\mathrm{d}v}{\mathrm{d}t} = \frac{\mathrm{d}}{\mathrm{d}t}(mv) \tag{2.7}$$

This form is convenient if we are dealing with a body of finite mass, but in fluid mechanics we are generally concerned with the steady flow of a continuous quantity of fluid. Here is it more convenient to work in terms of a flux of momentum, M, defined as the product of the **mass flowrate** w and the velocity v:

$$M = wv = A\rho v^2 \tag{2.8}$$

Thus if we consider a control volume as shown in Fig. 2.4 we can say that the

difference between the flowrates of momentum into and out of the volume will be the rate of change of momentum and hence equal to the net force on the control volume.

The forces on the control volume are the pressure forces at the two cross-sections, which are given by the product of the area and the absolute pressure, A_1P_1 and A_2P_2, and the net force F exerted by the wall of the duct on the fluid. This is equal and opposite to the force exerted by the fluid on the inside surface of the duct. Summing these forces and applying Newton's Law gives

$$A_1P_1 - A_2P_2 - F = M_2 - M_1 \tag{2.9}$$

or

$$F = \left(A_1P_1 + A_1\rho_1v_1^2\right) - \left(A_2P_2 + A_2\rho_2v_2^2\right) \tag{2.10}$$

Note that in the derivation of this equation we have not needed to make the assumption that the density is constant. Unlike Bernoulli's equation, this is valid for compressible as well as incompressible fluids. Furthermore, we have not needed to assume loss-free flow and as a result this equation is more generally valid than Bernoulli's equation. Note also that as the two pressures P_1 and P_2 are multiplied by different areas, it is essential that absolute pressure values are used. This point is considered in greater detail in Example 2.4 below.

We shall illustrate the use of these three basic equations by means of a set of examples.

EXAMPLE 2.1: SMALL ORIFICE IN THE SIDE OF A LARGE TANK

Figure 2.5 shows the system under investigation, in which a fluid is flowing through an orifice at a depth H below the surface of a fluid. Applying Bernoulli's equation from a point on the top surface to the jet emerging from the orifice, we can assemble our data as follows. Consider a control surface extending from the top surface to the jet and let section 1 be a point on the top surface. The pressure here is atmospheric, and as the velocity is small we can say that $P_1 = P_a$, where P_a is atmospheric pressure, $v_1 \simeq 0$. We can take the orifice as our datum of height, and therefore $h_1 = H$.

Within the jet the pressure is again atmospheric, as we can neglect the variation of atmospheric pressure with height as a result of the small density of air. The velocity is the unknown v and the height is at the datum. Hence

$$P_2 = P_a, \qquad v_2 = v \qquad \text{and} \qquad h_2 = 0 \tag{2.11}$$

Substituting these quantities into Bernoulli's equation gives

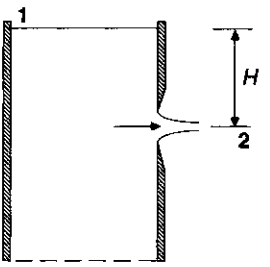

Fig. 2.5 Example 2.1: flow through an orifice at depth H below the surface of fluid in a tank.

$$\frac{P_a}{\rho} + \frac{0^2}{2} + gH = \frac{P_a}{\rho} + \frac{v^2}{2} + 0 \tag{2.12}$$

or

$$v = \sqrt{2gH} \tag{2.13}$$

We have calculated this velocity on the assumption that there are no energy losses. In practice there will be some small losses due to drag on the wall near the orifice and rearrangements within the jet. Hence the velocity will be slightly less than the ideal value of equation (2.13). This reduction is commonly expresed in terms of a **velocity coefficient** C_v defined so that

$$v = C_v\sqrt{2gH} \tag{2.14}$$

Typical values for C_v in this geometry are about 0.98, suggesting that only about 4% of the total energy content is lost.

Observation of the jet shows that there is considerable contraction downstream of the orifice. This is *not* due to surface tension, as it occurs whether the jet is surrounded by air or water. It is due to the momentum of the fluid approaching the orifice from the side and overshooting. The minimum cross-section is known as the ***vena contracta*** and its area is denoted by C_cA_o, where A_o is the area of the orifice and C_c is known as the **contraction coefficient**. For a single orifice, as shown in Fig. 2.5, C_c is often about 0.65 except at very low flowrates.

Equation (2.13) gives the velocity at the *vena contracta*, as it is in the parallel-sided part of the jet that the pressure is atmospheric. Thus the volumetric flowrate is given by

$$\begin{aligned} w_L &= C_cA_oC_v\sqrt{2gH} \\ &= C_DA_o\sqrt{2gH} \end{aligned} \tag{2.15}$$

where C_D is a **discharge coefficient** defined as the ratio of the actual

flowrate to that predicted on the assumption of no energy loss and no contraction. For the simple orifice, $C_D = C_c C_v$ and will be about 0.63.

Thus if we were to consider a hole of diameter 10 mm at a depth of 0.8 m below the top of a tank, we could predict the ideal velocity from equation (2.13) as

$$(2 \times 9.81 \times 0.8)^{0.5} = 3.96\,\mathrm{m\,s^{-1}}$$

Assuming a velocity coefficient of 0.98, the actual velocity would be $0.98 \times 3.96 = 3.88\,\mathrm{m\,s^{-1}}$. The orifice area is $\pi \times 0.01^2/4 = 7.85 \times 10^{-5}\,\mathrm{m^2}$, so that the area of the *vena contracta* will be about $0.65 \times 7.85 \times 10^{-5} = 5.11 \times 10^{-5}\,\mathrm{m^2}$. The mass flowrate will thus be given by equation (2.3) as $1000 \times 5.11 \times 10^{-5} \times 3.88 = 0.198\,\mathrm{kg\,s^{-1}}$.

EXAMPLE 2.2: THE ORIFICE PLATE

One of the commonest ways of measuring the flowrate in a pipe is to insert an orifice plate, as shown in Fig. 2.6. Normally there are three pressure tappings: one some way upstream of the plate, which we will call tapping 1; one near to the *vena contracta*, tapping 2; and one some way downstream of the orifice plate, tapping 3. Unfortunately the UK and US codes of practice do not agree about the best positions for these tappings. The UK code recommends tappings in the corner formed by the junction of the orifice plate with the tube wall, whereas the US code recommends close to the *vena contracta* and a few diameters upstream of the orifice. Whatever their merits for flow measurement, the US tappings are more convenient for theoretical analysis and will be considered here.

Observations using dye traces in transparent tubes show that the flow is smooth as far as the *vena contracta*, suggesting loss-free flow, whereas downstream of the *vena contracta* the jet breaks up, inducing gross eddies with consequential energy losses. It takes some considerable distance before smooth flow is re-established. In the present analysis we shall assume that tapping 2 is at the *vena contracta*, tapping 1 is sufficiently far upstream for the flow to be unaffected by the presence of the orifice, and tapping 3 is sufficiently far downsteam for smooth flow to be re-established.

If the system is ideal we can assume that there are no energy losses between sections 1 and 2 and apply the continuity and Bernoulli equations, giving

$$w = A_1 v_1 \rho = A_2 v_2 \rho \tag{2.16}$$

and

$$\frac{P_1}{\rho} + \frac{v_1^2}{2} = \frac{P_2}{\rho} + \frac{v_2^2}{2} \tag{2.17}$$

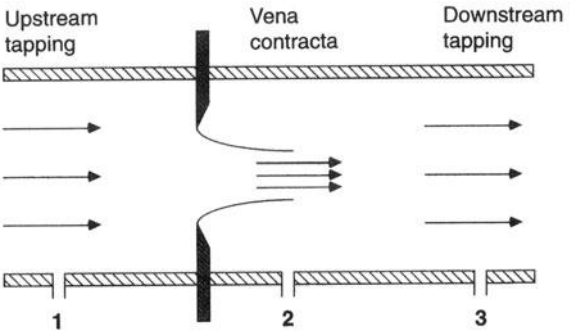

Fig. 2.6 Example 2.2: the orifice plate, showing pressure tappings.

Eliminating v_1 and v_2 between these equations gives

$$w = A_2\left[\frac{2\rho(P_1 - P_2)}{1-\left(\frac{A_2}{A_1}\right)^2}\right]^{1/2} \tag{2.18}$$

However, we must bear in mind that this analysis neglects the loss of energy, and that A_2 is the area of the *vena contracta* and not the orifice area. As in Example 2.1, the former effect causes little in the way of error, but the jet contraction does have a major effect on the result. The area A_2 can be written as C_cA_o, where A_o is the area of the orifice. We could therefore replace A_2 by C_cA_o in equation (2.18), giving

$$w = C_cA_o\left[\frac{2\rho(P_1 - P_2)}{1-\left(\frac{C_cA_o}{A_1}\right)^2}\right]^{1/2} \tag{2.19}$$

but it is more usual to write this equation in the form

$$w = C_DA_o\left[\frac{2\rho(P_1 - P_2)}{1-\left(\frac{A_o}{A_1}\right)^2}\right]^{1/2} \tag{2.20}$$

where C_D is not quite equal to C_c, not only because of the existence of a velocity coefficient due to energy losses, but also because C_c has been

omitted from the fraction within the square root. Because the orifice plate is the one of the commonest methods of measuring flowrate, the values of C_D have been determined with the greatest care, and extensive tabulations of C_D as a function of Reynolds number and area ratio can be found in the BSI publication on flow measurement (BS 1042). In conjunction with the values obtained from these tables an orifice plate can give very high accuracy and is often used as the standard for calibrating other flow-measuring devices.

We cannot use Bernoulli's equation to predict the pressure P_3 downstream of the orifice plate as there is considerable eddying as the jet breaks up, with corresponding loss of energy. Instead we can use the momentum equation, together with the assumption that there is negligible longitudinal force on this short section of the pipe. Thus the applied force is given by

$$A_1(P_2 - P_3)$$

which must equal the momentum change, $w(v_3 - v_2) = A_1\rho v_1(v_3 - v_2)$. Thus

$$P_3 - P_2 = \rho v_1(v_2 - v_1) \tag{2.21}$$

where we have replaced v_3 by v_1 as almost always the pipe diameters before and after the orifice are equal. Note that as $v_2 > v_1$, the pressure rises downstream of the orifice plate. Comparison with equation (2.19) shows that the pressure rise after the orifice plate does not equal the pressure drop between sections 1 and 2. Thus combining equations (2.18) and (2.21) predicts that there is an overall pressure loss given by

$$P_1 - P_3 = \frac{1}{2}\rho(v_2 - v_1)^2 \tag{2.22}$$

which can alternatively be written as

$$P_1 - P_3 = \frac{1}{2}\frac{w^2}{\rho}\left(\frac{1}{A_2} - \frac{1}{A_1}\right)^2 \tag{2.23}$$

The overall pressure loss is proportional to the square of the flowrate w, and this is typical of the pressure drop across any item of plant, such as a sudden change in pipe diameter, a pipe bend or a valve.

If we have water flowing with a velocity of $1.5\,m\,s^{-1}$ in a tube of diameter 30 mm fitted with an orifice of diameter 20 mm, we can calculate the relevant areas by $A_1 = A_3 = \pi \times 0.03^2/4 = 7.07 \times 10^{-4}\,m^2$ and $A_2 = 0.65 \times \pi \times 0.02^2/4 = 2.04 \times 10^{-4}\,m^2$, assuming a contraction coefficient of 0.65. The velocity v_2 is given from equation (2.16) as $1.5 \times 7.07 \times 10^{-4}/2.04 \times 10^{-4} = 5.20\,m\,s^{-1}$. Thus from equation (2.17) the pressure drop $P_1 - P_2 = 1000 \times (5.20^2 - 1.5^2)/2 = 12.4\,kN\,m^{-2}$ and the pressure recovery downstream of the orifice is, from equation (2.21), $1000 \times 1.5 \times (5.20 - 1.5) = 5.55\,kN\,m^{-2}$. There is therefore an overall pressure loss of $12.4 - 5.55 = 6.8\,kN\,m^{-2}$.

EXAMPLE 2.3: THE VENTURI TUBE

The Venturi tube is a modified version of the orifice plate that has the advantage of a lower overall pressure loss. It consists of a smooth contraction in the cross-section of a pipe followed by a gradual expansion back to the original area. The pressure is measured upstream of the contraction, P_1, and at the throat, P_2, as shown in Fig. 2.7. It is also of interest to predict the pressure P_3 downstream of the Venturi. The expanding part of the Venturi is known as the **diffuser**, and observations show that if the angle of divergence is less than about 10° the jet does not break away from the walls of the diffuser, and smooth (and therefore nearly loss-free) flow occurs.

The analysis given in the previous section for the pressure drop $P_1 - P_2$ still applies but now, because of the gradual contraction of the tube, there is little tendency for the jet to contract further and the discharge coefficient differs only slightly from unity, this being due mainly to the effects of wall friction. Furthermore, as the jet does not break away from the edge of the orifice, little energy is lost downstream of the throat and the pressure recovery $P_3 - P_2$ is only marginally less than the pressure drop. Thus there is little overall pressure drop across the device as a whole, and a Venturi tube is therefore to be preferred to an orifice plate whenever there is a need to maintain the presure. However, Venturi tubes are long, owing to the small diffuser angle, and need to be machined with care in order to maintain loss-free flow. Orifice plates are easy to make and, being only a few millimetres in width, can easily be slipped between existing pipe flanges. In many circumstances, particularly for liquids, the extra pumping costs associated with the pressure drop across an orifice plate are quite negligible and the greater ease of construction and convenience of installation make the orifice plate the more popular of the two devices.

EXAMPLE 2.4: FORCE ON A PIPE BEND

Let us consider as an example a contracting section of pipe that is bent through 180°, as shown in Fig. 2.8. If the pipe is short and smooth-walled

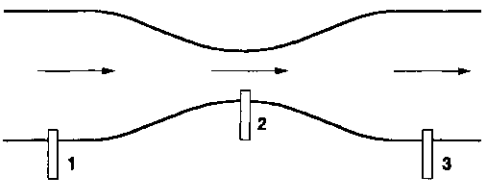

Fig. 2.7 Example 2.3: the Venturi tube, showing pressure tappings.

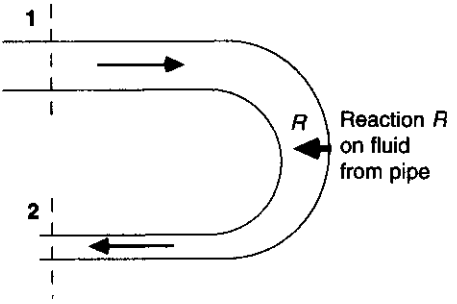

Fig. 2.8 Example 2.4: force on a bend.

there will be little loss of energy and we can apply Bernoulli's equation from inlet to outlet as follows:

$$\frac{P_1}{\rho}+\frac{v_1^2}{2}=\frac{P_2}{\rho}+\frac{v_2^2}{2} \tag{2.24}$$

The applied forces on the fluid within the pipe are

1. the forces on the end section, A_1P_1 and A_2P_2, which act to the right, and
2. the force R exerted by the inside surface of the pipe on the fluid. This force acts on the fluid to the left and is equal and opposite to the force exerted by the fluid on the pipe wall.

The sum of the forces, $A_1P_1 + A_2P_2 - R$, must equal the net creation of rightward momentum. The inlet momentum through section 1 is $wv_1 = A_1\rho v_1^2$; leftward momentum leaves section 2 at the rate $A_2\rho v_2^2$.

Thus the rate of creation of rightward momentum is $-A_1\rho v_1^2 - A_2\rho v_2^2$, and

$$R=\left(A_1P_1+A_1\rho v_1^2\right)+\left(A_2P_2+A_2\rho v_2^2\right) \tag{2.25}$$

Comparing this with equation (2.9) reveals that we have a difference in sign, and this results from the 180° bend in the tube. Indeed we can note that the impulse function $\boldsymbol{F}$, defined as $(AP + A\rho v^2)$, is a vector and must be added accordingly:

$$\boldsymbol{R}=\boldsymbol{F}_1+\boldsymbol{F}_2 \tag{2.26}$$

There remains a small complication, however. In principle, the pressures in the equations of this section should be absolute pressures, as it is the absolute pressure times the area that gives rise to a force. We have however emphasized that $\boldsymbol{R}$ is the force on the inside surface of the pipe and there will be an additional force exerted by the surroundings on the

outside surface of the pipe. This equals atmospheric pressure, P_a, times the projected area, which in this case is $A_1 + A_2$, and acts from right to left. Thus the total force on the pipe, due to the fluids inside and outside the pipe, is given by

$$R_T = \left(A_1(P_1 - P_a) + A_1\rho v_1^2\right) + \left(A_2(P_2 - P_a) + A_2\rho v_2^2\right) \qquad (2.27)$$

We see therefore that in order to obtain the **total** force on the system, we must use gauge and not absolute pressures. This is intuitively reasonable as, if the gauge pressure is zero throughout, there is clearly no force on the duct.

Let us consider a duct that contracts from a cross-sectional area A_1 of $4 \times 10^{-3}\,m^2$ to A_2 of $2 \times 10^{-3}\,m^2$ while being bent through an angle of 60°, as shown in Fig. 2.9. Water discharges to atmosphere at section 2 with a velocity of $10\,m\,s^{-1}$.

From continuity, we can say that $v_1 = v_2A_2/A_1 = 5\,m\,s^{-1}$. As the fluid discharges to atmosphere at section 2, the gauge pressure $P_2 = 0$, and from Bernoulli's equation

$$P_1 = P_2 + \frac{\rho}{2}(v_2^2 - v_1^2) = 37.5\,kN\,m^{-2}$$

The impulse function at section 1 is given by

$$F_1 = A_1(P_1 + \rho v_1^2) = 250\,N$$

and

$$F_2 = A_2(P_2 + \rho v_2^2) = 200\,N$$

Both these impulse functions act on the control surface, as shown in Fig. 2.9. The net force to the right, X, is given by $X = 250 - 200\cos 60° = 150\,N$ and the net upward force $Y = 200\sin 60° = 173\,N$. The resultant force $R = (150^2 + 173^2)^{0.5} = 229\,N$ and acts at an angle $\tan^{-1}(173/150) = 49°$ to the horizontal.

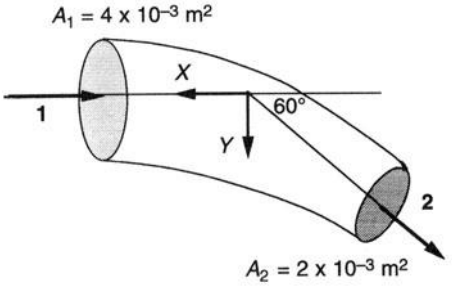

Fig. 2.9 Example 2.4: pipe bend through 60°.

2.3 Laminar flows

2.3.1 Introduction

At low Reynolds numbers the flow is **laminar** and, as shown in Fig. 2.2, the assumption that the velocity is uniform across the duct is untenable. In particular, it is found that the velocity in contact with a stationary solid surface is zero. This is often called the **no-slip condition**. The critical Reynolds number below which laminar flow occurs depends on the geometry of the situation, but in a pipe of circular cross-section the critical Reynolds number is about 2200. Reynolds numbers below this critical value are commonly encountered in the more viscous liquids of the food industry.

In laminar flow the effects of **viscosity** are dominant. By definition the viscosity μ is the constant of proportionality between the shear stress τ and the velocity gradient dv/dy:

$$\tau = \mu \frac{dv}{dy} \tag{2.28}$$

This is most conveniently illustrated by considering two parallel planes a distance Y apart as in Fig. 2.10. The lower plate is held stationary and the upper plate is moved with velocity v. The velocity gradient is v/Y and hence the shear stress on the upper plate is $\mu v/Y$. Thus the force F required to maintain the motion is $A\mu v/Y$, where A is the area of the plate. Viscosity is the resistance of a fluid to distortion; fluids such as Golden Syrup have high viscosity in comparison to water. It takes its name from *viscum*, the Latin for mistletoe, because of the stickiness of the berries. If the viscosity μ is constant (that is, not a function of either τ or dv/dy), the fluid is said to be **Newtonian**. Non-Newtonian fluids will be discussed in Chapter 5.

The viscosity can be measured in a variety of commercially available viscometers, each type being appropriate for a particular range of viscosities. This too will be discussed in greater detail in Chapter 5. Viscos-

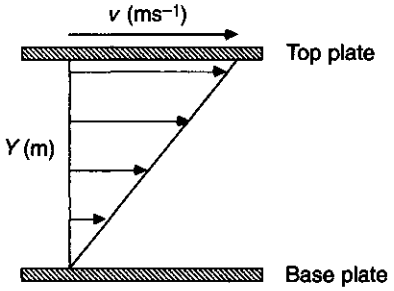

Fig. 2.10 Effect of viscosity: flow between parallel plates Y apart where the top plate moves at velocity v.

ity is a very important physical parameter, which controls the behaviour of laminar flows. Non-Newtonian fluids have more complex flow properties as a result of μ not being a constant. This section, however, only describes the behaviour of Newtonian fluids.

Viscosity is, however, a strong function of temperature, as anyone who has warmed syrup will know, and indeed engine-lubricating oils contain special additives in an attempt to limit this variation. In solutions, the viscosity is also a function of concentration. Thus when looking up tabulated values of viscosity, it is essential to ensure that the data are at the required temperature.

In many simple geometries, the velocity distribution and the associated pressure gradient can be obtained by a simple force balance, similar to that employed in the derivation of the momentum equation, and the definition of the viscosity. We shall illustrate the method by a single example.

2.3.2 *Laminar flow in a tube of circular cross-section*

We shall consider a fluid of viscosity μ flowing in a tube of radius R and length L under the influence of an overall pressure difference of magnitude ΔP. As the pressure gradient $\mathrm{d}P/\mathrm{d}l$ is uniform along the tube it will equal $\Delta P/L$. We can find the shear stress τ at an arbitrary radius r from the centreline of the tube by considering a force balance on a cylindrical element of radius r and length δl as shown in Fig. 2.11. The difference between the forces on the two ends of the element, $\pi r^2(\mathrm{d}P/\mathrm{d}l)\delta l$, must equal the force on the side of the element $2\pi r\tau\delta l$:

$$\pi r^2 \frac{\mathrm{d}P}{\mathrm{d}l}\delta l = 2\pi r\tau\delta l \tag{2.29}$$

where τ is the **shear stress**; that is, the shear force acting per unit area of the curved surface of the element. Equation (2.29) can be rewritten to give τ as

$$\tau = \frac{r}{2}\frac{\mathrm{d}P}{\mathrm{d}l} \tag{2.30}$$

By the definition of a Newtonian fluid, however, the shear stress can also be written as

$$\tau = \mu\frac{\mathrm{d}v}{\mathrm{d}r} \tag{2.31}$$

as $\mathrm{d}v/\mathrm{d}r$ is the velocity gradient perpendicular to the surface on which τ acts. Combining equations (2.30) and (2.31) gives

$$\mu\frac{\mathrm{d}v}{\mathrm{d}r} = \frac{r}{2}\frac{\mathrm{d}P}{\mathrm{d}l} \tag{2.32}$$

and on integrating equation (2.32) with respect to r we have

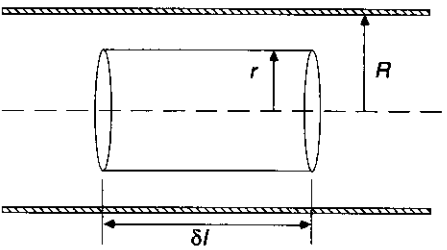

Fig. 2.11 Laminar flow in a tube of circular cross-section, radius R, showing section of radius r.

$$\mu v = \frac{r^2}{4}\frac{dP}{dl} + A \tag{2.33}$$

where A is an arbitrary constant of integration. The constant A can be evaluated from the no-slip condition, that the velocity must be zero on the tube wall, i.e. that $v = 0$ on $r = R$. Hence

$$A = -\frac{R^2}{4}\frac{dP}{dl} \tag{2.34}$$

and, substituting for A into equation (2.33),

$$\mu v = \frac{\left(r^2 - R^2\right)}{4}\frac{dP}{dl} \tag{2.35}$$

The volumetric flowrate w_L can be found from the integral of the product of the velocity with the elementary area $2\pi r\, dr$:

$$w_L = \int_0^R v 2\pi r dr \tag{2.36}$$

or

$$w_L = -\frac{\pi R^4}{8\mu}\frac{dP}{dl} \tag{2.37}$$

The minus sign appearing, perhaps unexpectedly, in this equation is necessary as the pressure gradient dP/dl is formally a negative quantity, because the fluid flows in the direction of decreasing pressure. Equation (2.37) can also be expressed in terms of the mean velocity v_m defined by

$$w_L = \pi R^2 v_m \tag{2.38}$$

giving

$$v_m = -\frac{R^2}{8\mu}\frac{dP}{dl} \tag{2.39}$$

Substituting this equation into equation (2.35) gives

$$v = 2v_m\left[1 - \left(\frac{r}{R}\right)^2\right] \tag{2.40}$$

which is the equation quoted in section 2.1.3 and plotted in Fig. 2.2. Clearly the velocity profile is parabolic. Furthermore, by putting $r = 0$, it can be seen that the centreline velocity v_1 is twice the mean velocity v_m, as already noted in that section.

This type of analysis can be carried out in a wide range of simple geometries. For example, in a rectangular slot of width w and thickness b, where $b \ll w$, the result corresponding to equation (2.35) is

$$\mu v = \frac{\left(4y^2 - b^2\right)}{8}\frac{dP}{dl} \tag{2.41}$$

where y is distance from the central plane, and equation (2.38) becomes

$$w_L = -\frac{b^3 w}{12\mu}\frac{dP}{dl} = bwv_m \tag{2.42}$$

The velocity profile is given by

$$v = 1.5v_m\left[1 - \left(\frac{2y}{b}\right)^2\right] = v_1\left[1 - \left(\frac{2y}{b}\right)^2\right] \tag{2.43}$$

Again, the profile is parabolic but, in this case, the mean velocity is two thirds of the centreline velocity.

Velocity profiles such as these are typical for all Newtonian fluids, including many food fluids. Thus when a food fluid flows down a pipe, different parts of the fluid will spend different lengths of time within the pipe. Thus, if cooking or sterilization is taking place, some parts of the fluid will be processed for longer times than others. This effect will give rise to uneven processing, and will be discussed further in Chapter 8 in the context of residence time distributions.

The equations derived above can be manipulated into a different form, which we shall find convenient in section 2.5. We can see from equation (2.29) that the magnitude of the shear stress on the wall, τ_w, is given by

$$\tau_w = -\frac{R}{2}\frac{dP}{dl} \tag{2.44}$$

and hence we can rewrite equation (2.39) in the form

$$\tau_w = \frac{16\mu v_m}{R} \tag{2.45}$$

Both sides of this equation can be divided by $\frac{1}{2}\rho v_m^2$ to give

$$\frac{\tau_w}{\frac{1}{2}\rho v_m^2} = 16\frac{\mu}{\rho v_m(2R)} \tag{2.46}$$

This is traditionally written in the form

$$c_f = \frac{16}{Re} \tag{2.47}$$

where the friction factor c_f is defined by

$$c_f = \frac{\tau_w}{\frac{1}{2}\rho v_m^2} \tag{2.48}$$

and Re is the conventional Reynolds number. In this form we can make direct comparison with the corresponding results for turbulent flow, which will be presented in section 2.5. Correlations for the friction factor are very useful for predicting the pressure drop needed to pump a fluid along a pipe, and thus are important in the design of process plant.

EXAMPLE 2.5

Consider $0.6\,l\,s^{-1}$ of a fluid of viscosity $0.015\,N\,s\,m^{-2}$ flowing in a 50 mm diameter pipe: the mean velocity can thus be evaluated as $0.6 \times 10^{-3} \times 4/(\pi \times 0.05^2) = 0.306\,m\,s^{-1}$. Assuming a density of about $1000\,kg\,m^{-3}$, the Reynolds number will be $0.306 \times 0.05 \times 1000/0.015 = 1019$. This is well below the critical value of 2200 and laminar flow will therefore occur.

From equation (2.37) the pressure gradient is given by $-8 \times 0.015 \times 0.6 \times 10^{-3}/(\pi \times 0.025^4) = -58.7\,N\,m^{-3}$. Thus if the pipe is 15 m long, the pressure drop will be $15 \times 58.7 = 881\,N\,m^{-2}$. The centreline velocity will be twice the mean velocity, i.e. $0.612\,m\,s^{-1}$, so that some fluid will spend only $15/0.612 = 24.5$ s within the pipe compared with the mean residence time of twice this value, 49 s.

2.3.3 *Flow through packed beds*

In the food industry, it is often important to calculate the pressure drops through filters or membranes that consist of arrays of solid particles. These are both examples of flow through packed beds, a topic that was first studied in 1846 by Darcy, the gardening consultant for Dijon City Council, who was interested in the right sort of gravel to put round his fountains. Darcy's book (*Les Fontaines Publiques de la Ville de Dijon,* Paris, 1856) is generally regarded as the first serious study of fluid mechanics, and his conclusion, that the pressure gradient through a packed bed is directly proportional to the flowrate w_L, is commonly known as **Darcy's law**:

$$\frac{dP}{dl} \propto w_L \tag{2.49}$$

More detailed analysis by Carman and Kozeny, treated in texts such as Kay and Nedderman (1985), gives rise to the following result for beds composed of spherical particles:

$$\frac{dP}{dl} = \frac{180\mu v(1-\varepsilon)^2}{D^2\varepsilon^3} \tag{2.50}$$

where v is the superficial velocity, i.e. the volumetric flowrate per unit area of bed (w_L/A), D is the diameter of the particles and ε is the void fraction, i.e. the volumetric fraction of the bed occupied by the fluid. In the case of non-spherical particles or particles of mixed sizes an equivalent spherical diameter must be used and a shape factor has to be included. Details of these are given in Kay and Nedderman (1985).

The constant of proportionality between the superficial velocity and the pressure gradient is sometimes called the **permeability**. It is noteworthy that this is both inversely proportional to the square of the particle diameter and very sensitive to the void fraction. The permeability is proportional to $\varepsilon^3/(1-\varepsilon)^2$, i.e. roughly proportional to ε^5. Thus a small degree of compaction of the bed greatly decreases the permeability; for example, a 2% change in voidage causes a 10% change in the permeability.

The Carman–Kozeny equation (2.50) gives an excellent prediction of the pressure gradient provided the Reynolds number, here defined by

$$Re' = \frac{dv\rho}{\mu(1-\varepsilon)} \tag{2.51}$$

is less than about 10. At higher Reynolds numbers allowance must be made for inertial effects, and an extra term has to be inserted into equation (2.50), giving the result known as the **Ergun correlation**:

$$\frac{dP}{dl} = \frac{150\mu v(1-\varepsilon)^2}{d^2\varepsilon^3} + \frac{1.75\rho v^2(1-\varepsilon)}{d\varepsilon^3} \tag{2.52}$$

where ρ is the density of the fluid. This correlation is generally regarded as the best available. The discrepancy between the constant of 180 in the Carman–Kozeny equation and the 150 in the Ergun correlation is not easily explained away, and may be taken as an indication of the precision of these results. Again the extreme sensitivity of the pressure gradient to the void fraction should be noted.

EXAMPLE 2.6

We can calculate the pressure difference required to force water of viscosity $0.89 \times 10^{-3}\,\mathrm{N\,s\,m^{-2}}$ at $0.01\,\mathrm{m\,s^{-1}}$ through a filter cake of thickness 5 mm consisting of 20 μm spherical particles, packed to a voidage of 0.4.

First we must evaluate the Reynolds number, which in this case is

$$20\times10^{-6}\times0.01\times\frac{1000}{0.89\times10^{-3}\times(1-0.4)}=0.375$$

which is well below the critical value of 10, enabling us to use the Carman–Kozeny equation. Thus from equation (2.50)

$$\frac{dP}{dl}=\frac{180\times0.89\times10^{-3}\times0.01\times(1-0.4)^2}{(20\times10^{-6})^2\times0.4^3}=2.25\times10^7\ \mathrm{Nm^{-3}}$$

The pressure drop ΔP is $2.25\times10^7\times0.005=1.13$ bar.

It is also instructive to consider gravity-driven flows, such as a fluid flowing vertically downwards through a filter. Here the fluid will be driven not only by any applied pressure gradient but also by its own weight. Thus we must modify the pressure gradient terms in equations (2.50) and (2.52) to $dP/dl+\rho g$.

EXAMPLE 2.7

Let us consider the flow of water through a sand filter consisting of a 50 mm thick layer of 400 μm spherical grains packed to a voidage of 0.4. If the depth of water above the bed is 15 cm, we can say that the pressure at the top of the bed will be $0.15\times1000\times9.81=1472\ \mathrm{Nm^{-2}}$, and hence the pressure gradient will be $1472/0.05=29430\ \mathrm{Nm^{-3}}$. Using the Ergun equation, (2.52), as we cannot be confident that the Reynolds number is below 10, we have

$$29430+1000\times9.81=\frac{150\times0.89\times10^{-3}\times v\times(1-0.4)^2}{(400\times10^{-6})^2\times0.4^3}+\frac{1.75\times1000\times v^2\times(1-0.4)}{400\times10^{-6}\times0.4^3}$$

or

$$39240=4693000\ v+41020000\ v^2$$

from which we find that

$$v=7.82\times10^{-3}\ \mathrm{ms^{-1}}$$

The Reynolds number of the flow is

$$\frac{7.82\times10^{-3}\times400\times10^{-6}\times1000}{0.89\times10^{-3}\times(1-0.4)}=5.86$$

showing that the use of the Ergun equation was unnecessarily complicated, and that it would have been sufficiently accurate to use the simpler Carman–Kozeny equation.

2.4 Dimensional analysis

2.4.1 Introduction

We noted in the previous sections that laminar flows in simple geometries can be analysed from first principles but that there is as yet no equally fundamental understanding of turbulent flow or of the processes of heat and mass transfer. Such topics must be investigated experimentally. The technique of dimensional analysis can be of the greatest help in minimizing the number of necessary experiments and in the determination of the most convenient and general presentation of the results. In particular, dimensional analysis permits us to deduce the behaviour of full-sized plant from tests on scale models.

2.4.2 Buckingham's theorem

The concept of dimensional analysis is based on the fact that the dimensions of all the terms in an equation must be the same. For example, distances are conventionally measured in miles and time in hours. Thus speed, which is calculated by dividing distance by time, must have the units of miles per hour. This principle of dimensional consistency is of the greatest value when considering scale-up and model tests, and consequently it is used widely throughout engineering science and is particularly useful in fluid mechanics. We should emphasize the difference between dimensional consistency, as discussed above, which is a physical requirement, and the use of consistent, preferably SI, units which is an arithmetical necessity.

First, we must decide what constitutes an independent dimension. This is a somewhat subjective matter but international convention recognizes seven independent dimensions of which **mass**, **length**, **time**, **temperature** and **quantity of material** are relevant to fluid mechanics and transfer processes. (The other two, electric current and luminous intensity, are of no interest in this context.) In the absence of heat and mass transfer, only mass, length and time are important and these will be denoted by M, L and T respectively. In the SI system, quantities with these dimensions are expressed with the units of kilograms, metres and seconds.

The need for dimensional consistency imposes as many constraints on the form of our equations as there are independent dimensions. This idea is formalized in Buckingham's theorem, which states that any relationship between M parameters, containing between them n independent dimensions, can be expressed in terms of $(M - n)$ dimensionless groups. This concept has similarities with the phase rule, which may be familiar from elementary chemistry.

We can illustrate the use of dimensional analysis by considering the force F exerted by a flowing stream on a sphere of diameter D. We can assume that the force on the sphere depends on the mean velocity of the fluid v_m

and the fluid properties, density ρ and viscosity μ as well as on its diameter. Thus

$$F = f(D, v_m, \rho, \mu) \tag{2.53}$$

The dimensions of these quantities are

F	D	v_m	ρ	μ
$\left(\frac{ML}{T^2}\right)$	(L)	$\left(\frac{L}{T}\right)$	$\left(\frac{M}{T^3}\right)$	$\left(\frac{M}{LT}\right)$

We see that three fundamental dimensions are involved: our five parameters can thus be expressed in terms of $(5 - 3) = 2$ dimensionless groups. There are many ways of obtaining these groups. Perhaps the most straightforward is to select two parameters of particular interest, F and μ say, and make these dimensionless by dividing by powers of the remaining parameters. Thus if we take $F/\rho^\alpha D^\beta v_m^\gamma$, we can determine its dimensions as $(ML/T^2)(L^3/M)^\alpha(1/L)^\beta(T/L)^\gamma$. The whole group must be dimensionless and therefore we can equate the indices of each dimension to zero.
Thus

$$\text{for M} \quad 1 - \alpha = 0 \tag{2.54}$$

$$\text{for T} \quad -2 + \gamma = 0 \tag{2.55}$$

$$\text{for L} \quad 1 + 3\alpha - \beta - \gamma = 0 \tag{2.56}$$

from which we find that $\alpha = 1$, $\gamma = 2$ and $\beta = 2$. Thus $F/\rho D^2 v_m^2$ is dimensionless. This is a useful parameter, which is called the drag coefficient c_D. (Take care not to confuse the drag coefficient with the discharge coefficient defined in Example 2.1.)

Similarly $\mu/\rho D v_m$ is dimensionless. However, this is the reciprocal of the familiar Reynolds number, which is traditionally used instead. Thus experimental data can be correlated in terms of c_D and Re. Confusingly, a constant of $8/\pi$ was inserted into the definition of the drag coefficient early in this century; it has been retained here to provide consistency with the classical results. Thus the drag coefficient and Reynolds numbers are usually defined by

$$c_D = \frac{8F}{\pi \rho D^2 v_m^2}$$

and

$$Re = \frac{v_m D \rho}{\mu} \tag{2.57}$$

These are clearly independent, as c_D is the only one to contain F and Re is the only one to contain μ.

We can therefore say that

$$c_D = f(Re) \qquad \text{only} \tag{2.58}$$

This result is exact if equation (2.53) is a complete list of the relevant parameters. The compilation of such lists therefore requires some physical insight. The final result also demonstrates why it is important to select the dimensionless groups with care. As an alternative to the use of c_D and Re we could have used the groups $F/\rho D^2 v_m^2$ and $F\rho/\mu^2$. This is mathematically correct, but inconvenient if the objective is to predict the force, as F appears in both groups. However, the latter formulation is more convenient for the prediction of the velocity resulting from a specified force.

In the absence of any theoretical prediction of the drag on a sphere, a dimensionless formulation greatly simplifies experimental investigation and the resulting use of any data produced. Suppose we wanted to determine the dependence of the drag force on the other parameters (diameter, velocity, density and viscosity) experimentally. We would need to select about ten values of each and conduct a very large number of experiments. However, equation (2.58) shows that we need consider only one sphere and one fluid and conduct ten experiments at ten different velocities. It would, of course, be wise to perform one or two experiments with other fluids and another sphere just to confirm that our list of variables, equation (2.53), is complete. Such experiments have been performed many years ago and the set of equations

$$\begin{aligned} c_D &= \frac{24}{Re}\left(1 + 0.15\, Re^{0.687}\right) && Re < 1000 \\ c_D &= 0.44 && 1000 < Re < 10^5 \\ c_D &= 0.1 && Re < 10^5 \end{aligned} \tag{2.59}$$

has been found to be sufficiently accurate for most purposes. The experiments, however, show some inconsistent results for a range of Reynolds numbers close to 10^5, indicating that a parameter has been omitted from the list in equation (2.53). This turns out to be the surface roughness of the sphere, which makes a small difference to the values in the equations and a large difference in the critical Reynolds number for the sudden drop in c_D from 0.44 to 0.1. (This is why golf balls are dimpled. A well-struck golf ball will have a Reynolds number close to 10^5 and by roughening the surface the retarding force can be reduced by a factor of about 4, with obvious advantages.)

The Reynolds number is of particular interest in dimensional analysis as it controls the degree of turbulence and the flow pattern. It is usual to distinguish between **geometric similarity**, meaning of identical shape (that is, that ratios of lengths are the same) and **dynamic similarity** (ratios of forces are the same), which occurs at equal Reynolds numbers.

The same principles can be used to justify performing experiments on

scale models of any device of interest. We can illustrate this with the following example.

EXAMPLE 2.8

Suppose we have designed a new type of a tubular air cooler of overall length 8 m in which we intend to process 0.6 $m^3 s^{-1}$ of air. Before building it, let us make a $\frac{1}{10}$th scale model out of Perspex and use water to study the flow pattern. At the same time we can measure the pressure drop and hence predict the pressure drop that will occur in the full-size cooler.

The pressure drop ΔP will depend on the volumetric flowrate w_L, the length L and the fluid properties μ and ρ:

$$\Delta P = f(w_L, L, \mu, \rho) \tag{2.60}$$

We have five parameters and three dimensions giving two independent dimensionless groups. We cannot define a conventional Reynolds number as we know neither the diameter nor the velocity, but $w_L\rho/\mu L$ is dimensionless (the flow coefficient) and serves the same purpose. The other group must contain ΔP and, selecting ρ to eliminate the mass dimension, we find that $\Delta P/\rho$ has dimensions $(M/LT^2)(L^3/M) = L^2/T^2$, which are the dimensions of w_L^2/L^4.

Thus $\Delta P L^4/\rho w_L^2$ is dimensionless (the pressure coefficient) and therefore

$$\frac{\Delta P L^4}{\rho w_L^2} = f\left(\frac{w_L \rho}{\mu L}\right) \tag{2.61}$$

is an acceptable (but not the only) way of correlating the results.

Suppose that tests on the model give the following results:

w_L (ls^{-1})	1.0	2.0	4.0	6.0	8.0
ΔP (bar)	0.031	0.088	0.250	0.460	0.707

The properties of the two fluids are

Air	$\rho = 1.29\,kg\,m^{-3}$	$\mu = 1.71 \times 10^{-5}\,N\,s\,m^{-2}$
Water	$\rho = 1000\,kg\,m^{-3}$	$\mu = 0.89 \times 10^{-3}\,N\,s\,m^{-2}$

From these values we can calculate

$$\frac{w_L \rho}{\mu L} = \frac{1000 w_L}{0.89 \times 10^{-3} \times 0.8} = 1404 \times 10^3 w_L$$

$$\frac{\Delta P L^4}{\rho w_L^2} = \frac{\Delta P \times 0.8^4}{1000 w_L^2} = 4.096 \times 10^{-4} \Delta P / w_L^2$$

giving the following values:

$\frac{w_L\rho}{\mu L}$	1404	2808	5618	8427	11236
$\frac{\Delta PL^4}{\rho w_L^2}$	1.270	0.901	0.640	0.532	0.452×10^6

These dimensionless results are plotted in Fig. 2.12. They apply generally to all coolers of this design irrespective of size and for all fluids, unlike the raw data above, which are specific for one cooler and one fluid.

The full-size cooler is geometrically similar to the model. It operates with a value of

$$\frac{w_L\rho}{\mu L} = \frac{1.29 \times 0.6}{1.71 \times 10^{-5} \times 8.0} = 5658$$

From the graph the value of $\Delta PL^4/\rho w_L^2$ corresponding to this value of $w_L\rho/\mu L$ is seen to be 0.638×10^6, so that the value of the pressure drop in the full-size cooler is given by

$$\Delta P = \frac{0.638 \times 10^6 \times 1.29 \times 0.6^2}{8.0^4} = 72.3 \text{Nm}^{-2}$$

The method we have used above was for demonstration purposes. However, it involved an unnecessary amount of arithmetic, as we have calculated several points on the graph but only used one value. We could have saved arithmetic by saying

$$\text{If } \left(\frac{w_L\rho}{\mu L}\right)_{FS} = \left(\frac{w_L\rho}{\mu L}\right)_M, \qquad \text{then } \left(\frac{\Delta PL^4}{\rho w_L^2}\right)_{FS} = \left(\frac{\Delta PL^4}{\rho w_L^2}\right)_M$$

where the subscripts FS and M refer to the full-size and model respectively. Thus the 'equivalent flowrate' in the model, w_{LM}, is given by

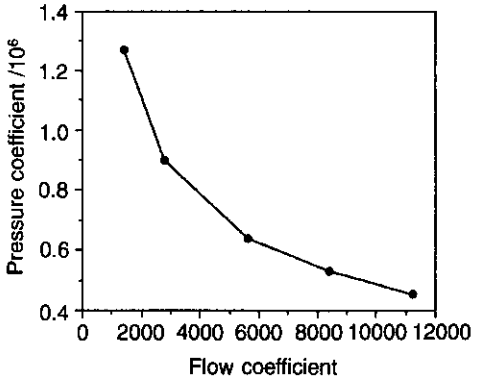

Fig. 2.12 Example 2.8: plot of dimensionless pressure coefficient versus flow coefficient.

$$w_{LM} = w_{LFS}\left(\frac{\rho_{FS} L_M \mu_M}{\rho_M L_{FS} \mu_{FS}}\right)$$

$$= 0.6 \times \frac{1.29}{1000} \times \frac{1}{10} \times \frac{0.89 \times 10^{-3}}{1.71 \times 10^{-5}} = 4.028 \times 10^{-3}\ \mathrm{m^3\,s^{-1}}$$

This is the only flow through the model that gives us any information about the behaviour of the full-sized cooler when operating at $0.6\,\mathrm{m^3 s^{-1}}$, as it is necessary that we have dynamic similarity, i.e. equality of Reynolds numbers.

By interpolating from the original table we find that the 'equivalent pressure drop' in the model $\Delta P_M = 0.252$ bar. But, since we have equated our Reynolds numbers, the other group must remain unchanged, and therefore

$$\left(\frac{\Delta P L^4}{\rho w_L^2}\right)_{FS} = \left(\frac{\Delta P L^4}{\rho w_L^2}\right)_M$$

Hence the pressure drop in the full-sized cooler is given by

$$\Delta P_{FS} = \Delta P_M \left(\frac{L_M}{L_{FS}}\right)^4 \frac{\rho_{FS}}{\rho_M} \left(\frac{w_{LFS}}{w_{LM}}\right)^2$$

$$= 0.252 \times 10^5 \times \left(\frac{1}{10}\right)^4 \times \frac{1.29}{1000} \times \left(\frac{0.6}{4.028 \times 10^{-3}}\right)^2$$

$$= 72.3\ \mathrm{N m^{-2}} \text{ as before}$$

The same principles can be used for a great variety of problems. Not only can they be used for the interpretation of model tests, but many correlations are most conveniently expressed in dimensionless form. This is particularly so in the study of heat and mass transfer, as will be evident in later chapters. Indeed, it is generally accepted that all valid correlations must be capable of being expressed in dimensionless form. The appearance of any experimentally determined dimensional constant in a correlation is usually taken to be proof that some parameter of importance has been neglected. This principle can usefully be applied when studying published work. In some cases dimensionality may turn out to result from a parameter, such as the acceleration due to gravity, which cannot readily be varied. For example, it would be perfectly possible to correlate the velocity v of a falling mass with the distance h through which the mass has fallen, using the correlation $v = 3.13\sqrt{h}$. The constant 3.13 has the dimensions $L^{1/2}/T$ and therefore cannot be universal. Elementary mechanics tells us that $v = \sqrt{2gh}$. The constant 2 is dimensionless and universal. The first form of the correlation is valid only on Earth, whereas the dimensionally correct form would be valid on all planets.

EXAMPLE 2.9

Let us evaluate the terminal velocity of a sphere of diameter 5 mm and density 1020 kg m^{-3} falling through a liquid of density 1000 kg m^{-3} and viscosity 0.015 N s m^{-2} (a pea in a thickish soup!). At the terminal velocity the drag force F must equal the weight minus the Archimedean upthrust:

$$F = \frac{\pi}{6} D^3 (\rho_s - \rho_f) g$$

and hence the drag coefficient is given by

$$c_D = \frac{4D(\rho_s - \rho_f)g}{3\rho_f v^2} \tag{2.62}$$

Assuming that the Reynolds number is less than 1000, we can use the first part of the correlation (2.59):

$$c_D = \frac{24}{Re}(1 + 0.15 Re^{0.687}) \tag{2.63}$$

This pair of equations is inconvenient for solution as we do not yet know the velocity v. They are put in more convenient form by multiplying both sides of equation (2.63) by Re^2, giving

$$\begin{aligned} 24Re(1 + 0.15Re^{0.687}) &= c_D Re^2 \\ &= \frac{4D(\rho_s - \rho_f)g}{3\rho_f v^2}\left(\frac{\rho_f D v}{\mu}\right)^2 = \frac{4D^3(\rho_s - \rho_f)\rho_f g}{3\mu^2} \\ &= \frac{4 \times 0.005^3 \times (1020 - 1000) \times 1000 \times 9.81}{3 \times 0.015^2} \end{aligned}$$

i.e.

$$24Re(1 + 0.15Re^{0.687}) = 145.33$$

which has solution $Re = 4.30$. Hence the terminal velocity is given by

$$4.30 \times \frac{0.015}{0.005 \times 1000} = 0.0129 \text{ m s}^{-1}$$

This sort of settling velocity is found in the two-phase solid–liquid food mixtures studied in Chapter 8.

2.5 Turbulent flow

2.5.1 Introduction

The theory of turbulent flow is not yet sufficiently advanced for purely theoretical prediction to be possible and we must resort to correlations of

experimental results, using the techniques of dimensional analysis, as outlined in section 2.4. However, for many aspects of turbulent pipe flow, the experiments have been carried out sufficiently often and with sufficient care that the resulting correlations may be considered to be more precise than is normally required in practical situations. The results can be used to predict pressure drops and flow velocities in realistic situations.

2.5.2 *The friction factor* c_f

A force balance on the full diameter D of an elementary length δl of horizontal pipe gives

$$\frac{\pi}{4} D^2 \delta P = \pi D \delta l \tau_w \tag{2.64}$$

or

$$\tau_w = \frac{D}{4} \frac{dP}{dl} \tag{2.65}$$

where τ_w is the wall shear stress, D is the pipe diameter and dP/dl is the pressure gradient. This result is seen to be equivalent to equation (2.44). Thus when correlating the frictional effects of a flow we can consider either τ_w or dP/dl. Traditionally the former is used, and we can say by inspection that the wall shear stress depends on the pipe diameter, the mean velocity v_m and the fluid properties ρ and μ. Thus

$$\tau_w = f(D, v_m, \rho, \mu) \tag{2.66}$$

There five parameters contain between them three dimensions and, following the arguments of section 2.4.2, can be expressed in terms of two independent dimensionless groups. The two usually chosen are the Reynolds number Re defined by

$$Re = \frac{D v_m \rho}{\mu} \tag{2.67}$$

and the friction factor c_f, which was introduced in section 2.3.2 and defined by equation (2.48):

$$c_f = \frac{\tau_w}{\frac{1}{2}\rho v_m^2} \tag{2.68}$$

This is sometimes known as **Fanning's friction factor**. The appearance of the factor of $\frac{1}{2}$ in the definition of the friction factor is due to misconceptions in the past, but needs to be retained to maintain consistency with published correlations.

The experimentally determined dependence of the friction factor on the Reynolds number for a smooth-walled tube is shown in Fig. 2.13; logarith-

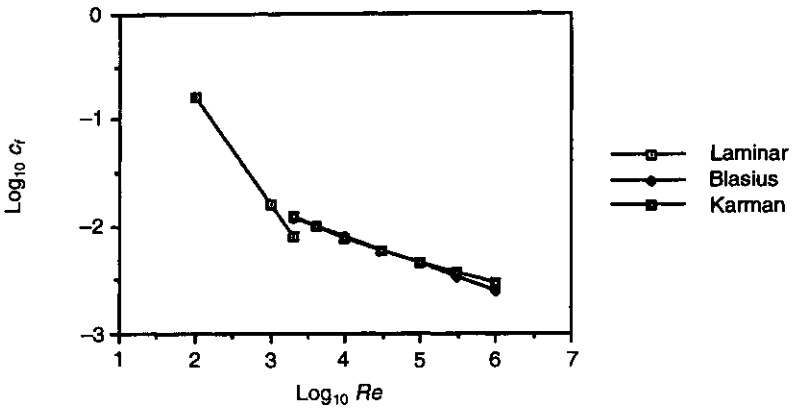

Fig. 2.13 Friction factor plotted against Reynolds number.

mic axes have been used in view of the wide range in the values of the Reynolds number. It is seen that there are two sections to the line, one for laminar flow at Reynolds numbers less than about 2000 and one for turbulent flow at greater Reynolds numbers. The effect of wall roughness is considered in section 2.5.4 below.

The theoretical prediction for laminar pipe flow, equation (2.37), can be rearranged to give

$$c_f = \frac{16}{Re} \tag{2.69}$$

This equation is exact for a Newtonian fluid, being derived from the definition of viscosity and geometrical arguments only.

For turbulent flow in a smooth-walled pipe, the experimental results lie on a gentle curve. However, for the range of Reynolds numbers normally encountered, it is sufficiently accurate to draw a best-fit straight line that has the form

$$c_f = 0.079\ Re^{-1/4} \tag{2.70}$$

and which is shown in Fig. 2.13. This equation is known as the **Blasius correlation** and is accurate to ±5% over the range $3000 < Re < 10^5$. For greater values of the Reynolds number the Karman–Nikuradse formula

$$\sqrt{\frac{1}{c_f}} = 1.74\ \ln\left(Re\sqrt{c_f}\right) - 0.40 \tag{2.71}$$

is more accurate but this is clearly of much less convenient algebraic form than the Blasius expression.

It can be seen from Fig. 2.13 that in turbulent flow the friction factor

normally lies in the narrow range $0.003 < c_f < 0.007$. Thus in the absence of more detailed information a rough guess of $c_f = 0.005$ is often sufficiently accurate for the prediction of pressure drops.

2.5.3 *Fanning's friction formula*

The flow in a pipe can be driven either by pressure difference or by change in elevation or by both. It is therefore more convenient to work in terms of loss of head as defined below. In a horizontal pipe the loss of head ΔH in a pipe of length L can be related to the pressure loss and pressure gradient by

$$\Delta H = \frac{\Delta P}{\rho g} = -\frac{1}{\rho g}\frac{\mathrm{d}P}{\mathrm{d}l}L \tag{2.72}$$

but if the pipe is inclined, allowance must be made for gravitational effects as in section 2.3.3. Thus it is appropriate to define the loss of head as

$$\Delta H = \frac{\Delta P}{\rho g} + \Delta h \tag{2.73}$$

where Δh is the decrease in elevation along the pipe: that is, the height of the pipe entry minus the height of the pipe exit. It is seen that, in this formulation, height and pressure are combined in exactly the same way as in Bernoulli's equation.

From equations (2.65), (2.68) and (2.73) we have

$$\Delta H = \frac{\Delta P}{\rho g} + \Delta h = \frac{4c_f v_m^2 L}{2gD} \tag{2.74}$$

This result is known as **Fanning's friction formula**.

As the velocity appears in this equation only as v_m^2, it seems that the head loss is independent of the sign of v_m. This is clearly incorrect as, if the flow were reversed, the sign of the head loss would be changed. Usually, however, the direction of the velocity is known and the sign of ΔH can be deduced by inspection.

We can illustrate the results of this section with a pair of examples.

EXAMPLE 2.10

Evaluate the pressure difference required to deliver $0.5\,\mathrm{l\,s^{-1}}$, i.e. $0.5 \times 10^{-3}\,\mathrm{m^3\,s^{-1}}$ of water through 100 m of 25 mm diameter pipe to a tank 4 m above the supply tank. The density and viscosity of water may be taken to be $1000\,\mathrm{kg\,m^{-3}}$ and $0.89 \times 10^{-3}\,\mathrm{N\,s\,m^{-2}}$.

The mean velocity is given by

$$v_m = \frac{4w_L}{\pi D^2} = \frac{4 \times 0.5 \times 10^{-3}}{\pi \times 0.025^2} = 1.019\ \mathrm{m\,s^{-1}}$$

and the Reynolds number by

$$Re = \frac{v_m D\rho}{\mu} = \frac{1.019 \times 0.025 \times 1000}{0.89 \times 10^{-3}} = 28624$$

As this value lies in the range in which the Blasius expression holds we have

$$c_f = 0.079 Re^{-1/4} = 0.079 \times (28624)^{-1/4} = 0.00607$$

Thus from equation (2.74):

$$\Delta H = \frac{4 \times 0.00607 \times 1.019^2 \times 100}{2 \times 9.81 \times 0.025} = 5.14\,\text{m}$$

Recalling that we have an **increase** in elevation of 4 m so that $\Delta h = -4$, we have from equation (2.73)

$$\Delta P = (5.14 + 4) \times 1000 \times 9.81 = 0.897\,\text{bar}$$

The converse problem, of evaluating the flowrate from a known value of the pressure drop, results in marginally more difficult arithmetic, as illustrated below.

EXAMPLE 2.11

Find the flowrate of water through 230 m of 50 mm diameter pipe under the influence of a pressure drop of 0.6 bar.

The difficulty here is that we cannot as yet evaluate the friction factor. However, from the Blasius expression we can say

$$c_f = 0.079 \times \left(\frac{1000 \times 0.050 v_m}{0.89 \times 10^{-3}} \right)^{-1/4} = 0.00513\ v_m^{-1/4}$$

Thus, from Fanning's equation:

$$\frac{0.6 \times 10^5}{1000 \times 9.81} = \frac{4 \times 0.00513 v_m^{-1/4} v_m^2 \times 230}{2 \times 9.81 \times 0.05}$$

or

$$v_m^{7/4} = 1.271 \qquad \text{i.e.} \qquad v_m = 1.15\,\text{m s}^{-1}$$

The flowrate w_L is given by

$$w_L = \frac{\pi}{4} \times 0.05^2 \times 1.15 = 2.26\,\text{l s}^{-1}$$

It is important at this stage to check that the Reynolds number lies in the range for which the Blasius expression is valid.

From equation (2.67):

$$Re = \frac{0.05 \times 1.15 \times 1000}{0.89 \times 10^{-3}} = 6.5 \times 10^4$$

which is within the Blasius range, and therefore the calculation is appropriate.

2.5.4 *Rough and non-circular ducts*

The Blasius and Karman–Nikuradse formulae apply only for ducts with smooth walls. In reality, no wall is perfectly smooth, although many commercial pipes are sufficiently smooth for the Blasius expression to apply. This is a particular problem in the food industry, because of the frequent occurrence of fouling. Immediately after cleaning, a pipe will have a low value of the friction factor, but this will gradually increase during operation until the next cleaning phase occurs.

In general, the surface roughness can be characterized in terms of an experimentally determined quantity known as the **equivalent roughness size**, e. This is a measure of the average size of the irregularities on the tube wall, and the dependence of the friction factor on the roughness is given by the empirical Colebrook formula:

$$\frac{1}{\sqrt{c_f}} = 3.46 - 1.74 \ln\left(\frac{2e}{D} + \frac{9.33}{Re\sqrt{c_f}}\right) \tag{2.75}$$

Typical values of the roughness size for clean drawn tubing and commercial steel are 2×10^{-6} m and 5×10^{-5} m respectively, but it is very difficult to predict the effect of fouling on these values except by careful observation of similar situations.

As the Reynolds number increases, the last term in the Colebrook equation becomes progressively smaller, and the friction factor tends to an asymptote given by

$$\frac{1}{\sqrt{c_f}} = 3.46 - 1.74 \ln\left(\frac{2e}{D}\right) \tag{2.76}$$

Because of the awkward form of the Colebrook equation it is recommended that calculations are performed using either the Blasius expression or equation (2.76), and that the Colebrook equation (2.75) is then used to check that the assumptions are reasonable or to make minor adjustments to the friction factor.

For ducts of non-circular cross-section, the basic equations derived above can be used, at least in the turbulent flow regime, if the diameter D is replaced by the **hydraulic mean diameter** D_H defined by

$$D_H = \frac{4A}{P} \tag{2.77}$$

where A is the cross-sectional area of the duct and P is the wetted perimeter; that is, the length of the perimeter in contact with the flowing fluid. In this form the concept is applicable also to open channels, in which case the free top surface of the liquid is not included when evaluating the wetted perimeter. For a circular pipe, $A = \pi D^2/4$ and $P = \pi D$ and therefore from equation (2.77) we find that the hydraulic mean diameter is equal to the actual diameter. For a duct of square cross-section, the hydraulic mean diameter equals the length of the side.

Some authors use the **hydraulic mean radius** R_H defined as A/P. This is a confusing parameter! It is seen that the hydraulic mean radius is a **quarter** of the hydraulic mean diameter and, furthermore, for a circular pipe the hydraulic mean radius is not equal to the actual radius. The hydraulic mean radius should therefore be used with caution.

EXAMPLE 2.12

A pipe of length 100 m and diameter 150 mm has a height difference of 2 m between its ends. Evaluate the flow of water when it is running half full.

When half full the wetted perimeter P is $\pi D/2 = 0.2356$ m and the cross-sectional area A is $\pi D^2/8 = 0.00884\,m^2$. The hydraulic mean diameter is $4A/P = 0.150$ m, i.e. the same as the diameter. The friction factor is therefore given by equation (2.70) as $0.079 \times (0.89 \times 10^{-3}/0.150 \times 1000 \times v_m)^{1/4} = 3.90 \times 10^{-3}\, v_m^{-1/4}$. Hence, from equation (2.74):

$$0 + 2.0 = \frac{4 \times 3.90 \times 10^{-3} \times v_m^{7/4} \times 100}{2 \times 9.81 \times 0.150}$$

i.e. $v_m = 2.14\,m\,s^{-1}$. The volumetric flowrate is the product $Av_m = 0.00884 \times 2.14 = 0.0189\,m^3\,s^{-1}$.

These results can be contrasted with those for a semicircular pipe of the same dimensions. A will be unchanged but P will be $\pi D/2 + D = 0.3856$ m and hence $D_H = 4 \times 0.00884/0.3856 = 0.0917$ m. The friction factor will be

$$0.079 \times \left(\frac{0.89 \times 10^{-3}}{0.0917 \times 1000 \times v_m} \right)^{1/4} = 4.41 \times 10^{-3}\, v_m^{-1/4}$$

and hence the velocity is given by

$$0 + 2.0 = \frac{4 \times 4.41 \times 10^{-3} \times v_m^{7/4} \times 100}{2 \times 9.81 \times 0.0917}$$

i.e. $v_m = 1.50\,m\,s^{-1}$ and $w_L = 0.0133\,m^3\,s^{-1}$. The reduced flowrate results from the increased drag provided by the top surface of the semi-circular pipe.

2.5.5 *Pressure losses in bends and pipe fittings*

It is rare for pipework to be straight and free from fittings such as valves or sudden expansions and contractions. There will be pressure losses in all these items due to the formation of turbulent eddies. The example of an orifice plate has already been considered in Example 2.2, and many other situations can be analysed in a similar manner. Clearly, these losses must be taken into account when predicting the flow through the system.

As shown in Example 2.2, the pressure loss in a sudden pipe expansion or contraction is generally found to be proportional to the square of the flowrate. Although this result was derived for ideal flow, it applies equally well when the flow is turbulent: that is, at high Reynolds numbers. Thus for any given fitting we can express the head loss as some multiple of the velocity head, $v^2/2g$. Typical values for the number of velocity heads lost in various fittings are given in the first column of Table 2.1. In addition we must remember that as a fluid enters a pipe from a large reservoir it will gain kinetic energy and there will be a corresponding reduction in the head of $v^2/2g$. Thus people often refer to an entry loss of one velocity head. (Strictly this is not a loss, as in principle the head could be recovered by fitting a diffuser. More pedantic authors refer to this as the 'unrecovered kinetic energy at exit'.)

Taking an approximate value for the friction factor of 0.005, we can see from equation (2.73) that the head lost in a pipe of length L is given by

$$\Delta H = \frac{4 \times 0.005 \times v_m^2 \times L}{2 \times g \times D} = \frac{0.02L}{D} \frac{v_m^2}{2g}$$

Thus there is a loss of one velocity head in a pipe of length $50D$. Hence the list of velocity heads lost given in Table 2.1 can also be expressed in terms

Table 2.1

	Number of velocity heads lost	Equivalent pipe length
90° standard bend	0.75	$38D$
90° large radius bend	0.45	$23D$
90° square or mitre bend	1.3	$65D$
T-junction		
straight through	0.4	$20D$
to or from side branch	1.0	$50D$
Gate valve		
open	0.17	$9D$
$\frac{3}{4}$ open	0.9	$45D$
$\frac{1}{2}$ open	4.5	$225D$
$\frac{1}{4}$ open	24.0	$1200D$
Swing check valve	2.0	$100D$

of an equivalent length of pipe. The use of these two alternative formulations will be illustrated in the problem below.

EXAMPLE 2.13

A typical domestic water supply consists of 20 m of 1.0 cm diameter pipe containing eight right-angled bends and a $\frac{3}{4}$ open gate valve. The water is supplied from a tank 8.0 m above the discharge point. Find the discharge rate.

Method of equivalent pipe lengths

The equivalent pipe length can be evaluated as follows:

Actual		20 m
Bends $8 \times 38\ D = 8 \times 38 \times 0.01$		3.04 m
Valve $45\ D = 45 \times 0.01$		0.45 m
Entry loss $50\ D = 50 \times 0.01$		0.50 m
	Total	23.99 m

Using equations (2.73) and (2.70) we have

$$8.0 = 4 \times 0.079 \left(\frac{0.89 \times 10^{-3}}{1000 \times v_m \times 0.01} \right)^{1/4} \frac{v_m^2 \times 23.99}{2 \times 9.81 \times 0.01}$$

which on rearranging becomes

$$v_m^{7/4} = 2.132 \qquad \text{or} \qquad v_m = 1.541\ \text{m s}^{-1}$$

Thus the volumetric flowrate is given by

$$w_L = \frac{\pi}{4} \times 0.01^2 \times 1.541 = 0.121\ \text{l s}^{-1}$$

We can evaluate the Reynolds number at this flowrate and use the Blasius expression to find the friction factor. This turns out to be 0.0069, which differs from the value of 0.005 assumed in the evaluation of the equivalent pipe lengths given in Table 2.1. Thus this method is inconsistent and its accuracy suspect. It is, however, very simple and can be recommended whenever great accuracy is not required. A better estimate can be obtained from the use of the tabulation of velocity heads as illustrated below.

Method of velocity heads

From Table 2.1 we see that we have a loss of 8×0.75 velocity heads in the bends, 0.9 in the valve and 1 at inlet, giving a total of 7.9 in addition to the frictional loss in the pipe.

Thus the lost head can be expressed by

$$\Delta H = \frac{4c_f v_m^2 L}{2gD} + 7.9\frac{v_m^2}{2g} \tag{2.78}$$

Putting in the values for this problem, we find that

$$8.0 = (8000c_f + 7.9)\frac{v_m^2}{2g} \tag{2.79}$$

Difficulties arise in the solution of this equation, as we cannot evaluate the friction factor until the velocity and hence the Reynolds number is known. The equation can be solved iteratively by

1. guessing a value for the friction factor;
2. substituting it into equation (2.79), evaluating the velocity and hence the Reynolds number; and
3. determining a better value for the friction factor.

This cycle can be repeated until convergence is achieved.

A value of 0.005 is always a good initial estimate for c_f. Thus

$$8.0 = (8000 \times 0.005 + 7.9)\frac{v_m^2}{2g}$$

from which we find that $v_m = 1.81\,\mathrm{m\,s^{-1}}$. We can now re-evaluate the friction factor using equation (2.70):

$$c_f = 0.079 \times \left(\frac{1.81 \times 0.01 \times 1000}{0.89 \times 10^{-3}}\right)^{-1/4} = 0.00662$$

Inserting this value into equation (2.79) gives $v_m = 1.61\,\mathrm{m\,s^{-1}}$, and reusing equation (2.70) gives $c_f = 0.00681$. This iteration can be repeated indefinitely and yields the following sequence of values for the velocity:

Iteration number	Velocity ($\mathrm{m\,s^{-1}}$)	Change in velocity ($\mathrm{m\,s^{-1}}$)
1	1.81	–
2	1.61	0.2
3	1.586	0.024
4	1.583	0.003

It can be seen that convergence is rapid, with each iteration making a change of about a tenth of the previous change. Thus an answer correct to about 1% can be obtained by the end of the third iteration, and further refinement is not warranted in view of the likely uncertainties in the data.

The value of $1.58\,\mathrm{m\,s^{-1}}$ differs only slightly from the previous estimate of

1.54 m s^{-1}. However, it is to be preferred as the concept of a lost velocity head has more generality than the concept of an equivalent pipe length.

2.5.6 *The one-seventh power law*

The velocity distribution in turbulent pipe flow is adequately described by the following empirical expression, which is known as the **one-seventh power law**:

$$v = v_1\left(\frac{y}{R}\right)^{1/7} \tag{2.80}$$

where v is the velocity at a distance y from the wall, R is the pipe radius and v_1 is the centreline velocity. This expression is found to be appropriate over the same range of Reynolds numbers as the Blasius equation and indeed the indices in these expressions can be derived from each other.

The mean velocity v_m can be evaluated as follows:

$$\pi R^2 v_m = \int_0^R 2\pi r v \mathrm{d}r = \int_0^R 2\pi(R-y)v_1\left(\frac{y}{R}\right)^{1/7}\mathrm{d}y \tag{2.81}$$

from which it follows that $v_m = \frac{49}{60}v_1$ or

$$v_1 = 1.22 v_m \tag{2.82}$$

The one-seventh power law has one major deficiency, in that it predicts an infinite velocity gradient at the wall. This can be seen by differentiating equation (2.80) to give

$$\frac{\mathrm{d}v}{\mathrm{d}y} = \frac{v_1}{7}R^{-1/7}y^{-6/7}$$

which gives $\mathrm{d}v/\mathrm{d}y = \infty$ when $y = 0$. This means that equation (2.80) cannot apply right up to the wall. However, it is found experimentally that turbulence is suppressed very close to a solid boundary and that a narrow laminar layer occurs between the wall and the turbulent core. This layer is known either as the viscous sublayer or the laminar sublayer and is of vital importance in the understanding of heat and mass transfer, as will become apparent in later chapters.

Within the laminar sublayer we can assume that the shear stress τ is given by

$$\tau = \mu\frac{\mathrm{d}v}{\mathrm{d}y} \tag{2.83}$$

provided the fluid is Newtonian. As the layer is thin and close to the wall we have that

$$v = \tau_w\frac{y}{\mu} \tag{2.84}$$

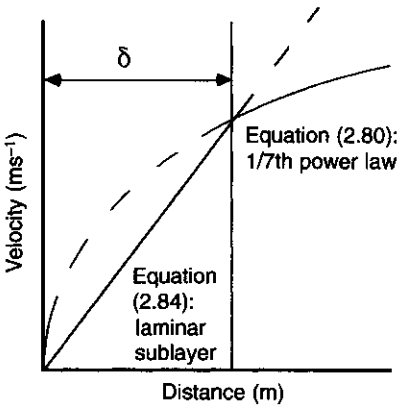

Fig. 2.14 The one-seventh power law, showing a laminar sublayer of thickness δ.

Equations (2.80) and (2.84) are sketched in Fig. 2.14 with the recommended profile being shown by the solid line. The evaluation of the thickness δ of the laminar sublayer is illustrated in the following example.

EXAMPLE 2.14

Find the laminar sublayer thickness for water flowing at a mean velocity of $1.5\,m\,s^{-1}$ *in a 2.0 cm diameter tube. The density and viscosity of water may be taken as* $1000\,kg\,m^{-3}$ *and* $0.89 \times 10^{-3}\,N\,s\,m^{-2}$.

The Reynolds number is given by

$$Re = \frac{1.5 \times 0.02 \times 1000}{0.89 \times 10^{-3}} = 33\,700$$

This lies within the range for which the Blasius expression is applicable, and we can therefore evaluate the friction factor as

$$c_f = 0.079 \times (33\,700)^{-1/4} = 0.00583$$

Thus, from the definition of the friction factor, the wall shear stress is

$$\tau_w = \frac{1}{2} \times 1000 \times 1.5^2 \times 0.00583 = 6.56\,N\,m^{-2}$$

From equation (2.84) the velocity profile in the laminar sublayer is given by

$$v = \frac{\tau_w y}{\mu} = \frac{6.56}{0.89 \times 10^{-3}} y = 7370y \qquad (2.85)$$

The centreline velocity of the water in the tube is given by equation (2.82):

$$v_1 = 1.22 \times 1.5 = 1.83\,\mathrm{m\,s^{-1}}$$

and thus from the one-seventh power law, equation (2.80), the velocity profile in the turbulent core is given by

$$v = 1.83\left(\frac{y}{0.01}\right)^{1/7} = 3.53y^{1/7} \qquad (2.86)$$

Equations (2.85) and (2.86) intersect at the edge of the laminar sublayer. The velocity predicted at that point must be the same for both equations. Hence the laminar sublayer thickness δ is given by eliminating v from these two equations:

$$3.53\ \delta^{1/7} = 7370\ \delta$$

from which we find that $\delta = 0.134\,\mathrm{mm}$.

It is noteworthy that the thickness of the laminar sublayer is of the order of 0.1 mm, a hundredth of the tube diameter. Thus the one-seventh power law is applicable for all but a very small fraction of the cross-section of the tube. It might therefore be thought that this parameter can be neglected. However, despite its very small thickness, the laminar sublayer plays a dominant role in heat and mass transfer, as will be discussed in Chapters 3 and 4. This is because it provides a zone across which heat and mass must be transferred by conduction or diffusion, both of which are molecular processes and therefore slow. Thus it provides a barrier between the wall and the effectively well-mixed turbulent core.

Conclusions

This chapter has introduced some of the basic ideas of fluid mechanics in order to help you understand how fluids move when they are pumped around or interact with solid particles (such as in a spray drier). Like the first chapter, the emphasis here has been to establish some essential principles and to show how these can be used. As noted in the introduction, many fluids – particularly liquids – in the food industry are viscous and non-Newtonian. Despite this, analysis based on ideal (non-viscous) and Newtonian (i.e. constant viscosity) fluids can be extremely useful, and this chapter is confined to such situations. You should understand the differences between an ideal and a real fluid, and appreciate how ideal fluids can often serve as a reasonable first basis for understanding the relations between flow and pressure, as well as explaining the principles of some common flow measurement techniques.

You should also understand: the differences between laminar and turbulent flows; how, for Newtonian fluids, the Reynolds number provides a basis

for discriminating between them; the profound implications of the flow regimes for velocity profiles and for flow/pressure drop relationships. You should also understand the importance of dimensional analysis in handling complex problems and how, with proper scaling, results can be extrapolated. Two typical operations are used as the basis for most of the presentation here. The first is the ubiquitous operation of pumping through pipes, where our emphasis is on ways of calculating the pressure (or head) requirements for a particular flow. The second covers some processes where the fluid either interacts with particles or flows through beds or porous filters.

Once again, this chapter can only scratch the surface of a huge field. Chapters 3 and 4, which deal with the processes of heat and mass transfer, will be found to rely on some of the principles and ideas developed here. Chapter 5 extends the discussion to more realistic fluid materials, in particular ones where the Newtonian assumption is not valid. Some ideas for further reading are listed below.

Further reading

There are mary basic texts on engineering fluid mechanics which descibe the material in this chapter in greater detail. A selection is listed below, although any good technical bookshop or library will contain many more.

Coulson, J.M. and Richardson, J.F. (1977) *Chemical Engineering*, Volume 1, Pergamon, London.

Kay, J.M. and Nedderman, R.M. (1985) *Fluid Mechanics and Transport Processes*, Cambridge University Press, Cambridge.

Tritton, D.J. (1988) *Physical Fluid Dynamics*, 2nd edn, Chapman & Hall, London.